Int. J. Heat Mass Transfer. Vol. 34, No. 7, pp. 1733–1745, 1991
Printed in Great Britain

0017–9310/91 $3.00 + 0.00

Measurement of three-dimensional temperature fields in conjugate conduction–convection problems using multidirectional interferometry

A. K. TOLPADI† and T. H. KUEHN
Department of Mechanical Engineering, University of Minnesota, Minneapolis, MN 55455-0111, U.S.A.

(*Received* 5 *July* 1988 *and in final form* 24 *August* 1990)

Abstract—A computational and experimental study is performed to optically record and reconstruct an asymmetric three-dimensional (3-D) temperature field in conjugate conduction–convection heat transfer problems. In a thermally coupled application, the temperature distribution must be obtained within the conducting solid and in the adjacent convecting fluid. A reconstruction algorithm is developed that provides the 3-D temperature field in a region occupied by multiple mediums (solids and/or fluids). The 3-D temperature distribution is reconstructed in and around a short heated cylinder placed in a fluid to which heat is transferred by natural convection. Experimental measurement of the field is made by recording and reducing the data from a number of interferograms taken along different angles to the flow. In order to obtain interference data through the combined solid and liquid, the refractive index of the cylinder is matched with the fluid. Numerical solutions for this geometry are also obtained which provide temperature fields that compare favorably with the experimentally obtained values.

INTRODUCTION

TEMPERATURE is a physical quantity the measurement of which is important. Several methods are available for measuring the temperature in fluids. Most of the techniques developed to date are invasive (e.g. thermometers, thermocouples, thermistors) requiring that a probe be inserted into the flow field. Such methods give the temperature only at specific locations in the fluid. Optical techniques, however, are very attractive because they are non-invasive and give the entire temperature field in real time. Low intensity light, being inertialess for all practical purposes, produces no disturbance in the flow field.

Interferometric methods for the study of two-dimensional (2-D) temperature fields in fluids have been widely known since the pioneering work of Eckert and Soehngen [1, 2]. A comprehensive review of optical methods in heat transfer is available in ref. [3]. For a 2-D field, a single interferogram contains all the necessary information, but for a three-dimensional (3-D) field, pathlength data is required along several directions of the refractive index (temperature) field. Data along each direction can be represented by an integral equation, and the 3-D problem reduces to the solution of a set of integral equations of the form

$$\phi_i = \int_0^s (n(x, y, z) - n_{\text{ref}})\, \mathrm{d}s_i \qquad (1)$$

where ϕ_i are the known pathlength data and $n(x, y, z)$ the unknown refractive index field.

The solution to this equation was considered in the area of radioastronomy by Bracewell and Riddle [4]. Subsequently it was applied to electron microscopy and X-ray imaging. Gordon *et al.* [5] proposed an iterative method of reconstruction called the Algebraic Reconstruction Technique (ART). An initial guess of the field is made that is successively improved with each iteration. This method is qualitative and is applicable even when limited data are available. It is well suited for Computer Assisted Tomography (CAT) scanners. In all these studies, the 3-D problem is reduced to a series of 2-D problems in parallel planes which are stacked together to form the entire 3-D field.

A mathematical method for the inversion of equation (1) as directly applicable to 3-D holography was first developed by Rowley [6]. A Fourier transform method was used that inherently requires information from a complete 180 deg field of view. Sweeney and Vest [7] have performed an exhaustive review of reconstruction algorithms. Six different schemes were compared: Fourier synthesis [6], Direct Inversion, Sinc method, Grid method, Frequency Plane Restoration and the ART method [5]. By assuming hypothetical refractive index fields, simulated interferometric data were generated. They found that redundant data were always required to obtain a good reconstruction. They parametrically varied the field of view and found that with a complete 180 deg field of view, all reconstruction schemes were accurate to within 1.5%. However, when the field of view was less than 180 deg, the Grid and Sinc methods gave the

† Present address: General Electric Research and Development Center, P.O. Box 8, Mail Stop K1/ES 206, Schenectady, NY 12301, U.S.A.

NOMENCLATURE

A_r aspect ratio of cylinder, L/D
D cylinder diameter
g gravitational acceleration
k thermal conductivity
l_x spacing between nodes in the x-direction, Fig. 1
l_y spacing between nodes in the y-direction, Fig. 1
L cylinder length
M number of sample points in the x-direction, Fig. 1
n index of refraction
N number of sample points in the y-direction, Fig. 1
Pr Prandtl number, ν/α
q strength of the line heat source, power per unit length
q' local heat flux, power per unit area
q^{**} dimensionless local heat flux, $q'D/k_{fl}[T_s - T_\infty]$
Ra_q Rayleigh number based on q, $g\beta qD^3/k_{fl}\nu\alpha$
T temperature
x dimensionless horizontal coordinate along the axis of the cylinder, X/D
y dimensionless horizontal coordinate perpendicular to the axis of the cylinder, Y/D
z dimensionless vertical coordinate measured upward from the centerline of the cylinder, Z/D.

Greek symbols

α thermal diffusivity
β volumetric coefficient of thermal expansion
Γ dimensionless temperature, $(T - T_\infty)k_{fl}/q$
θ angular coordinate measured from the top of the cylinder
θ_f angle of view, Fig. 1
λ_0 wavelength of light in vacuum
ν kinematic viscosity
ρ_i distance from the origin in the reconstruction plane, Fig. 1
ϕ_i pathlength.

Subscripts

fl fluid
num numerical
rec reconstructed
ref reference value
s cylinder surface
∞ bulk fluid.

best results. In each of these schemes, the rays were assumed to travel without refraction through the medium. Vest has reviewed tomographic reconstruction techniques for strongly refracting fields in ref. [8].

Based on the various reconstruction algorithms reviewed above, several experiments have been conducted to perform flow visualization studies and to measure 3-D refractive index fields. Matulka and Collins [9] used a holographic interferometer to study supersonic flow from a free jet. Using diffuser plates to scatter the light, interference patterns were recorded simultaneously on holographic plates. Chau and Zucker [10] obtained double exposure holograms of a 3-D refractive index field and used a thin laser beam to interrogate it to improve resolution. Vest and coworkers [11, 12] studied single and double natural convection plumes above heated surfaces in water. They reduced the holographic data in one horizontal plane using the Grid method in ref. [11] and the Sinc method in ref. [12]. Oertel [13] investigated cellular natural convection in a rectangular box. Interferograms were obtained along several directions in a shearing interferometer and the temperature field was reconstructed iteratively. Mayinger and Lubbe [14] constructed a holographic interferometer to study transient temperature fields during mixing of fluids in an octagonal test section. Double exposure holograms were recorded along four different directions and the ART method was used. Mewes and Ostendorf [15] studied the same phenomena in greater detail on the same setup. The fluid used was 95% dimethylsulphoxide which had an index of refraction that was matched with glass.

In all previous investigations, the temperature field in only one medium, i.e. a fluid, has been analyzed. An interesting and realistic situation occurs when the temperature field must be obtained in a conjugate conduction–convection problem. For such problems, the temperature field must be measured both in the solid and in the surrounding fluid simultaneously. In addition, if the field is three-dimensional, it is absolutely necessary to determine the complete temperature field to enable the calculation of the local heat flux distribution on the surface of the solid. With this in mind, a test problem of 3-D laminar natural convection around a short horizontal cylinder with a line heat source along the centerline was considered. A numerical solution to this problem was obtained using the finite difference code described in ref. [16]. Simulated pathlength measurements were obtained by integrating the solution along multiple directions. This

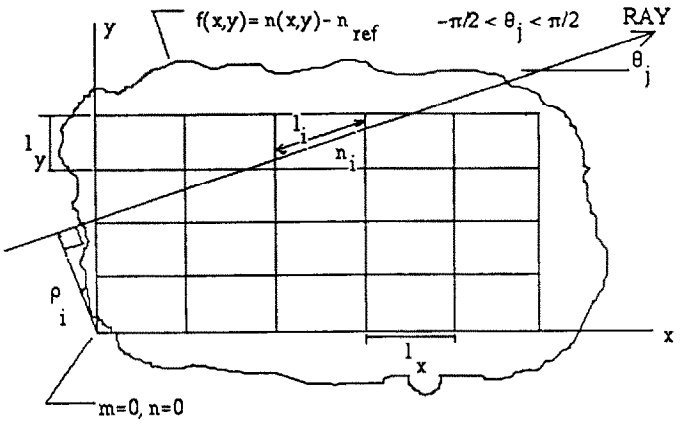

FIG. 1. Notation for the analysis of 3-D interferometric data.

was used to test an inversion algorithm for multiple mediums in the domain. Experimental data for this problem were obtained in a Mach–Zehnder interferometer (light source: He–Ne laser, $\lambda_0 = 0.6328$ μm). The cylinder was constructed of Plexiglas and was placed in a fluid having matched index of refraction. Interferograms of the temperature field were recorded along several directions and software was developed to digitize and process the fringe patterns. The 3-D temperature field was reconstructed using the inversion algorithm and was compared with the temperature field from the corresponding numerical solution.

RECONSTRUCTION METHOD

Single medium

Details of several reconstruction algorithms have been outlined in ref. [7] and will only be briefly summarized here. The pathlength ϕ_i is represented by equation (1) where $n(x, y, z)$ is the unknown refractive index field and n_{ref} the reference value of the refractive index. This integral is a line integral along the direction of the beam 's'.

For a three-dimensional refractive index field and in the *refractionless* limit, this equation can be solved by dividing the region into a series of parallel planes and obtaining a 2-D set of equations for each plane [7]. Three reconstruction methods were examined in the present study and the Grid method was found to give most satisfactory results.

With reference to Fig. 1, the Grid method involves the solution of the following system of linear algebraic equations, one for each plane

$$\sum_{m=0}^{M-1}\sum_{n=0}^{N-1} W_{mn}(\rho_i, \theta_j)[n(l_x m, l_y n) - n_{\text{ref}}] = \phi(\rho_i, \theta_j) \tag{2}$$

where the coefficients $W_{mn}(\rho_i, \theta_j)$ are related to the geometry and the grid which are detailed in ref. [7]. Here $n(l_x m, l_y n)$ is the unknown index of refraction at the node given by the location $x = l_x m$ and $y = l_y n$. $\phi(\rho_i, \theta_j)$ is the optical pathlength at location ρ_i along the ray direction θ_j.

As explained in ref. [7], it is important to have redundant data in obtaining a solution to the above system of equations. The problem is to determine the *best* possible solution. This solution will not, necessarily, satisfy every single equation but it would satisfy each as nearly as possible. The solution method used is a least squares regression.

A sensitivity analysis was made to study the effects of the number of angles of view and the number of data points per angle of view on the reconstruction error. Mathematical functions were used for the refractive index fields which were integrated exactly along a variety of 'rays' to generate simulated pathlength measurements. These were input into the reconstruction program from which the refractive index distributions were obtained. In keeping with the observation in ref. [7], it was found that redundant data were required to achieve a good reconstruction. The general observation was that the degree of redundancy should be between three and four, i.e. the amount of pathlength data required should be, at least, 3–4 times the total number of grid points.

Multiple mediums

In the previous section, the Grid method for reconstructing a refractive index field was outlined. If the relationship between the refractive index and the temperature is known, then the temperature field can also be obtained.

A special situation exists when the temperature field is required in a region that contains both a solid and a liquid. If the local heat flux distribution on the surface of the solid is desired, then the temperature field in the fluid in close proximity to the solid should be determined. From this, the temperature gradients normal to the surface can be computed which yields

the heat flux. In a 2-D problem, the solid region is often oriented such that its third dimension is in the direction of the light beam from which the temperature distribution in the entire fluid can be readily measured. In a 3-D case, multiple interferograms of the temperature field must be recorded. The integral information along the rays can be obtained with no difficulty in the fluid region, for instance in the plume above a heated body. However, if an opaque solid obstructs the light, the integral information through that part of the test region is lost. Therefore, the temperature field in the fluid adjacent to the solid cannot be retrieved from the interferograms. Thus, the temperature field can be reconstructed in any plane containing only the fluid, but it cannot be found in any plane passing through a portion of the solid.

It is necessary to have the index of refraction of the solid matched with the surrounding fluid when both mediums are present. The light will then pass through both the solid and the fluid with minimum refraction and interference fringes will be produced everywhere in the test region. The integral information in any plane intersecting the solid represents the combined effects of the solid and the fluid. The algorithm to invert the refractive index field in this situation is identical to the one described in the previous section with a minor difference. From the pathlength data (fringe order number), the 2-D refractive index distribution is obtained in any plane passing through the solid. The functional dependence of the refractive index on temperature must be known for both the solid and the fluid. Using these relationships, the temperature variation can be reconstructed simultaneously in the solid and the fluid.

In all the work done thus far, including that in ref. [7], only one medium has been considered. The temperature field was reconstructed in the fluid alone. Mewes and Ostendorf [15] who studied temperature fields in mixing of fluids did match the index of refraction of their glass stirrer with that of the surrounding medium. But, they made the assumption that the refractive index of glass changes very slightly with temperature and did not actually reconstruct the temperature field in the glass. To the knowledge of the authors, the work in ref. [15] is the only instance when the problem of refractive index matching was considered during the reconstruction of a 3-D temperature field.

The test geometry chosen is a short horizontal cylinder of aspect ratio unity with a line heat source along the centerline transferring heat to an infinite isothermal external fluid by laminar natural convection. Since the inversion technique is very involved, it was felt that a simple geometry should be considered initially to prove the concept. This geometry was selected for three reasons—the cylinder is easy to machine, it produces a 3-D temperature field that is desired for a test of the method and numerical solutions for this configuration can be easily obtained for comparison.

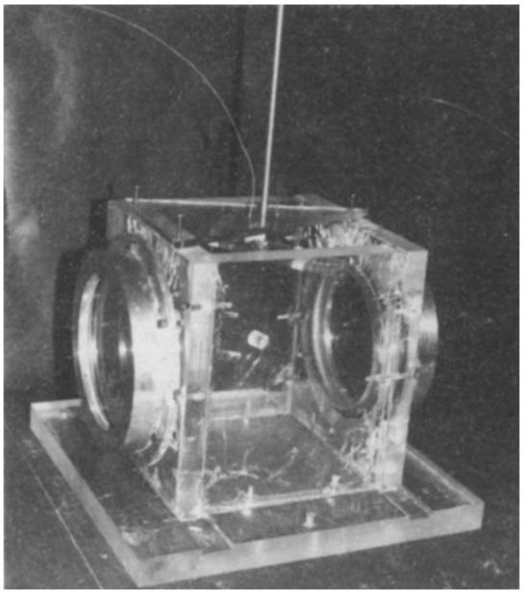

FIG. 2. Photograph showing the assembled test cell, cylinder and cylinder support mechanism.

EXPERIMENTAL STUDY

Apparatus

The cylinder was made of Plexiglas—1.27 cm in diameter and 1.27 cm in length. A 0.04 cm diameter hole was drilled along the centerline. A 0.0254 cm chromel heater wire (45 Ω m $^{-1}$) was placed in the hole and lead wires were soldered to the two ends for voltage and current taps. The cylinder was placed in a test cell which was filled with dibutylphthalate (DBP), a liquid the refractive index of which matched the Plexiglas. The cylinder was annealed at a temperature of 52°C (125°F) in an oven to minimize any residual internal stresses.

A rectangular test cell, constructed of 2.54 cm Plexiglas, contained the DBP surrounding the cylinder. The inside dimensions of the cell were 15.5 cm wide, 15.5 cm long and 20.5 cm high. Two holes were bored on the opposite sides of the cell to hold a pair of custom made 5.08 cm thick optical windows. The assumption made is that the test cell is large enough for the walls to have no effect on the flow and heat transfer around the cylinder. A simple support system was fabricated from which the cylinder was suspended and could be rotated to different angles in a horizontal plane. While taking data, the test cell was surrounded by styrofoam insulation of 6.35 cm thickness. Figure 2 shows the supporting system and cylinder placed in the test cell.

Soft 0.63 cm copper tubing was bent to form several turns of a water carrying heat exchanger that was placed in the test cell. This was located along the side walls, bottom of the test cell and just below the top surface of the fluid. The tubing was connected to a temperature controlled circulator bath the setting of which could be used to control the temperature of the

bulk DBP. Power to the cylinder heater wire was applied using a regulated d.c. power supply via a simple potentiometer. Two multimeters were used to measure the current through and the voltage applied across the heater. Interferograms were recorded on a Technical Pan film (a variable ASA high contrast film) using an 80–200 mm variable focal length lens and a Mach–Zehnder Interferometer (MZI) at the University of Minnesota Heat Transfer Laboratory.

The five physical properties of DBP that were required are density, specific heat capacity, viscosity, thermal conductivity and refractive index at 0.6328 μm. All these properties were independently measured over the temperature range 10–40°C using appropriate standard instruments. The corresponding properties of Plexiglas were obtained from the manufacturer's data sheet.

The property measurements indicated that the index of refraction of the solid and the fluid were equal at a temperature of 25.1°C. To confirm this result, simple finite fringe experiments were conducted by placing an unheated Plexiglas cylinder in an isothermal fluid. The matching temperature from these tests was found to be 25.1°C. At this temperature, the light was found to practically traverse through the solid and fluid without deflection except for a region of discontinuity near the interfaces and at the centerline where the heater wire was installed.

Procedure

Before any experimental data were taken, the interferometer was aligned such that the measuring beam was horizontal. Details on the adjustment procedure are available, for instance, in ref. [3]. The test cell was filled with fluid and the cylinder was lowered into it. The orientation of the cylinder could be adjusted with leveling screws on the support mechanism. It could also be adjusted by moving the lead wires vertically. By blocking the reference beam and observing the measuring beam alone in the camera, the cylinder was adjusted such that its axis was horizontal. Styrofoam insulation was placed around the test cell. The circulator bath was set to a temperature corresponding to the index matching temperature, 25.1°C. The test cell was left for over 24 h in an effort to bring the cylinder and fluid to an isothermal state. The temperature of the bath was constantly monitored until steady state was attained.

A finite fringe technique was used in recording all the interference data. The direction of the light beam in the MZI was fixed. In order to obtain interferometric data in several directions, the cylinder was rotated in steps of 10 deg and an interferogram was recorded at each position. Relatively, the beam would traverse the test region along different directions with respect to the cylinder. With the cylinder positioned at one angle, the interferometer mirrors were adjusted to produce horizontal fringes through the fluid and solid. A photograph of the fringe pattern was taken after an isothermal condition was reached. The power to the cylinder heater wire was then turned on, which caused a deviation of the fringe pattern. Without readjusting the interferometer, the fringe pattern was photographed after steady state was attained which took 3–4 h. The current flowing through the heater wire, the voltage applied, the circulator bath setting, and the fluid temperature were all recorded. The power was then switched off and the cylinder rotated 10 deg. The same cycle of operations was repeated for this new position of the cylinder. The power applied to the heater and the temperature of the fluid were maintained at the same value as before. Using this method, pairs of interference fringes were obtained for each orientation of the cylinder—one before applying power to the heater and another after turning the power on. The pathlength information for each angle is retrieved by performing a subtraction of the fringe locations in the two interferograms. Data were recorded at different angles over a 90 deg range. Figure 3 shows an example of a pair of fringe patterns with the cylinder axis oriented 20 deg from the light beam.

The processing of a large number of interferograms necessitated the use of an image digitizer. The digitizer that was utilized is one that is primarily being used for processing star images and has a specific capability of studying 35 mm negatives. Scanning is performed by a flying laser spot 12 μm in diameter. The digital output was recorded on the hard disk of a PDP-11/34 host computer and was subsequently transferred to a magnetic tape. These data were transferred from the tape to a VAX computer. Software was written to read the data, recover the coordinate information and perform polynomial curve-fits through the fringes. This was done with each of the two fringe patterns—obtained before and after heating. From the two sets of curve-fit data, the corresponding locations of a particular fringe in each view were subtracted. From this, the distribution of the fringe order number ε and thus the pathlength data ϕ were obtained. By defining a set of horizontal planes through the test region, the fringe order number (pathlength) distribution in each plane was computed using a linear interpolation of the data along the original fringes.

The fringe data in the fluid region above the cylinder were analyzed using the digitizer. However, in planes containing the solid, the amount of noise present in the fringe data was so great (e.g. Fig. 3) that it could not be analyzed digitally but was done manually.

The grid inversion algorithm described previously was used to reconstruct the temperature field in several horizontal planes from the experimentally obtained pathlength distribution. A more detailed description of the experimental set-up and procedure may be found in ref. [17].

RESULTS

A numerical solution was generated for this geometry using the generalized code described in refs. [16, 17]. The solution was obtained under conditions

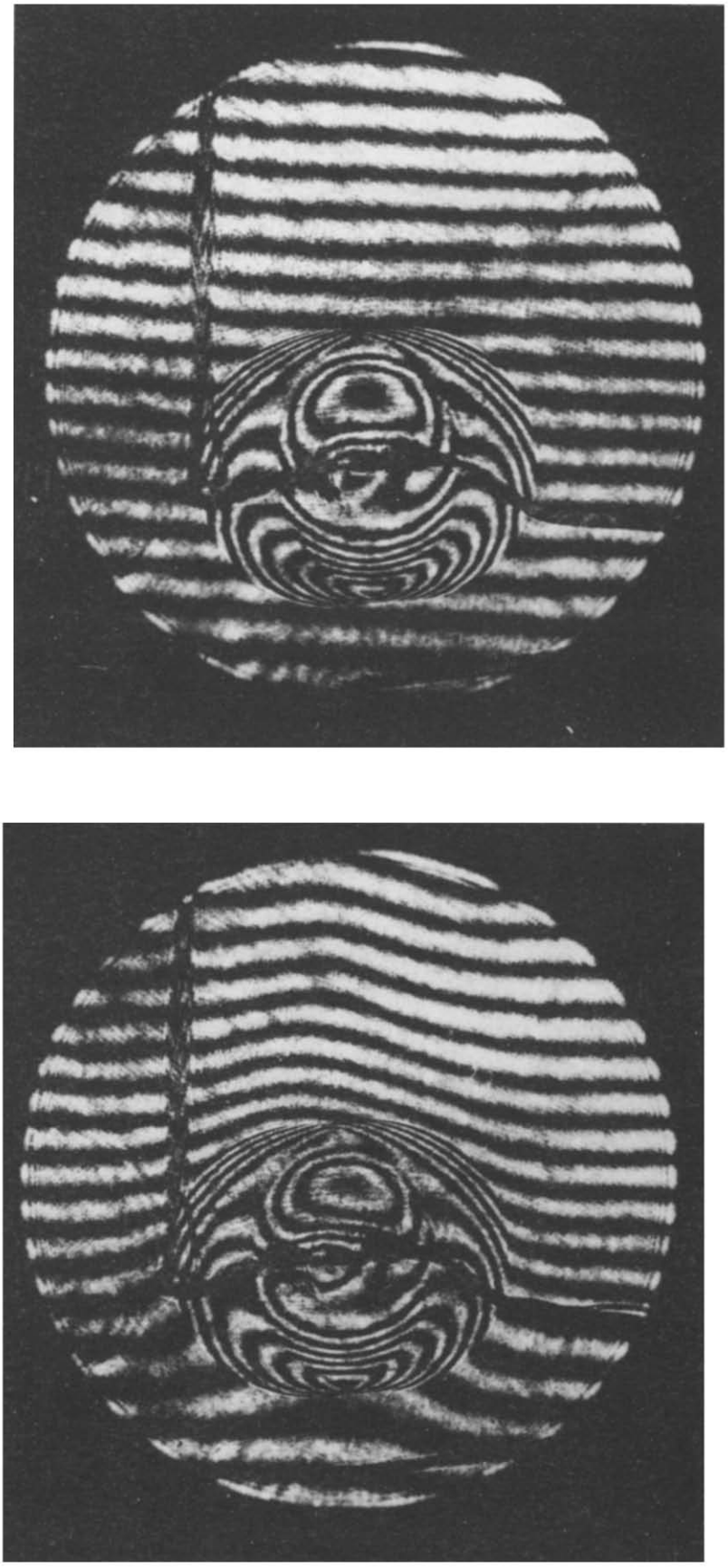

FIG. 3. Finite fringe patterns with the cylinder axis oriented 20 deg with respect to the light beam. The upper interferogram is taken with the cylinder unheated and the lower interferogram is recorded with the cylinder heated.

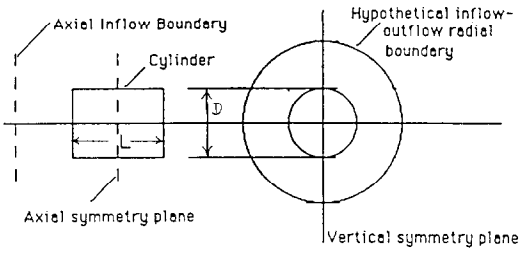

FIG. 4. Computational domain for a numerical solution for the short heated cylinder.

that corresponded to the actual experiments. The computational domain for this problem is indicated in Fig. 4. It is bounded in the angular direction by vertical top and bottom symmetry planes, in the axial direction by a vertical symmetry plane passing through the center of the cylinder and a hypothetically positioned axial inflow boundary, and in the radial direction, by the centerline and a hypothetical inflow–outflow boundary. The magnitude of the heating along the centerline used in the experiments was $q = 0.583$ W m^{-1}. Based on the properties of DBP under the conditions of the experiments (viscosity = 0.02082 kg m^{-1} s^{-1}, density = 1046 kg m^{-3}, thermal conductivity = 0.1466 W m^{-1} K^{-1}, specific heat = 1840 J kg^{-1} K^{-1}) this corresponded to a Rayleigh number, $Ra_q = 3.98 \times 10^4$. The Prandtl number of the fluid at a bulk temperature of 25°C is $Pr = 261.3$. This would imply a very thick hydrodynamic boundary layer compared to the thermal boundary layer. Tests were performed to study the effects of the grid spacing and the locations of the radial and axial outer boundaries on the solution. The grid that was found to be suitable for the problem was nonuniform having 17 points in the radial direction, 12 points in the angular direction and 17 nodes in the axial direction. The grid spacing was small in both of the radial and axial directions close to the cylinder to resolve the boundary layers and was made progressively larger in the outer regions of the domain. The minimum grid spacing in the radial and axial directions was 0.04 cylinder diameters adjacent to the cylinder. The outer boundaries were located 17.85 cylinder diameters away from the center in the radial direction and 15.45 cylinder diameters away in the axial direction, respectively.

The numerical solution was used as the basis for testing the Grid reconstruction method for multiple mediums. Several horizontal reconstruction planes were located, some through the cylinder and the fluid surrounding it while some contained only the fluid above or below the cylinder. A uniform rectangular grid was established in each plane. By selecting rays along several directions and performing numerical integrations along them, pathlength data were generated in each plane. This was used as input into the inversion algorithm from which the temperature field in each plane was reconstructed. An important point is that the temperature is continuous across a solid–fluid interface, but the temperature gradient is not, due to the differences in the thermal conductivity. Since the functional dependence of the index of refraction on temperature is different within the solid and the fluid, a discontinuity in the refractive index exists at the solid–fluid interface. The inversion technique should, therefore, have the capability of recovering the continuous temperature field from the discontinuous refractive index field.

Some of the results of the reconstruction are presented next. The grid used in these studies was a uniform 29×29 grid (841 points) in each horizontal plane. Over a 90 deg angle range, 16 equally spaced angles of view were chosen. For each angle of view, 125–135 equally spaced pathlength measurements were generated by integrating the numerical solution. This procedure was carried out for a set of horizontal planes, equally spaced in the vertical direction, some of them passing through the solid and some of them in the fluid region above or below the solid. The amount of pathlength data used in each plane, therefore, varied from 2000 (125×16) to 2160 (135×16). This provides a degree of redundancy of approximately 2.5. The amount of computational time required to perform a complete reconstruction of the temperature field in one plane using a 29×29 grid on a Cray-2 supercomputer was approximately 120 s. The majority of the computer time was spent in performing the matrix inversion, one for each plane.

It is useful to look at a typical reconstruction plane in relation to the cylinder. Figure 5 shows one such plane with the z-axis oriented parallel to the axis of the cylinder and the y- and z-axes placed perpendicular to the cylinder axis. The dimensionless temperature ($\Gamma = [T - T_\infty]k_{fl}/q$) distribution in a plane containing the center of the cylinder is portrayed in Fig. 6. The dotted curve represents the interface between the solid and the fluid. As expected, the highest temperature occurs along the axis of the cylinder where the heat source is located. The surface has an irregular appearance, and the temperature drops sharply in all directions from the center of the cylinder. The reconstruction should provide a temperature field that is symmetric about the origin which is the case in this figure. This serves as a good test of the reconstruction program. Since the thermal conductivity of the two mediums are not significantly different, the change in slope of the temperature field across the boundary is not evident. By calculating the differences between the reconstructed temperature field and the numerically computed temperature, the relative error ($[T_{rec} - T_{num}]/T_{num}$) distribution was obtained. The average relative error was found to be 3.05% with a standard deviation of 0.0351.

Figure 7 exhibits the temperature field in the plane

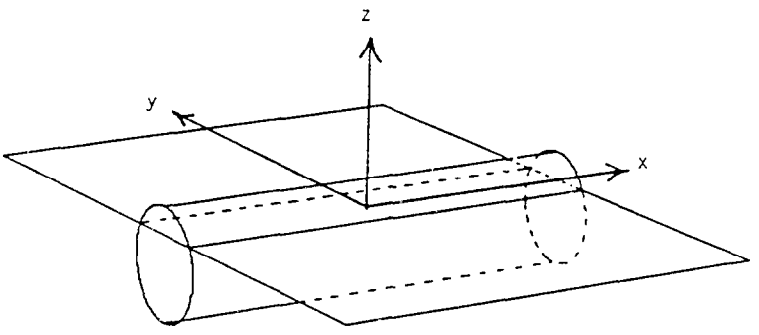

FIG. 5. Cylinder and a typical horizontal reconstruction plane.

0.1 diameters below the centerline of the cylinder. Comparing with Fig. 6, the temperature distribution is smoothed along the centerline and the irregularities are significantly reduced.

Considerable difficulties were encountered in analyzing the digitized data in cross-sectional planes passing through the solid. These problems were caused by the discontinuous interference fringes at the solid–liquid interface. This problem was alluded to earlier and is a consequence of several factors. Even though the bulk fluid was set to be at the correct matching temperature, the establishment of a temperature field created a situation that resulted in a mismatch of the refractive index in the majority of the solid fluid interface region. Even though the temperature was not significantly different from the matching temperature, it was sufficient to cause a discontinuity in the fringe pattern. Temperature mismatch on the cylinder surface caused refraction errors that resulted in fringe discontinuities. Moreover, there were interference patterns produced because of residual nonuniformities in the cylinder. Turning the cylinder in a lathe and drilling a hole along its axis were some operations that left residual stresses in the solid. This was minimized by annealing, but could not be eliminated entirely. Interference fringes are created by the stress patterns that are superimposed on those created by the temperature field. Another factor is that Plexiglas as a material is not entirely homogeneous. Plexiglas was chosen over glass because of its ease in machining, however, it suffers from the fact that its properties are somewhat dependent on the stock from which it is chosen. Therefore, the fringe data in planes containing the solid could not be reduced digitally but were performed manually by following the fringes.

The temperature distribution was obtained experimentally in a plane 0.1 cylinder diameters below the cylinder centerline. To achieve this, 55 pathlength measurements were used along each of the five different angles of view—0, 20, 40, 60 and 80 deg with respect to the axis of the cylinder. With this infor-

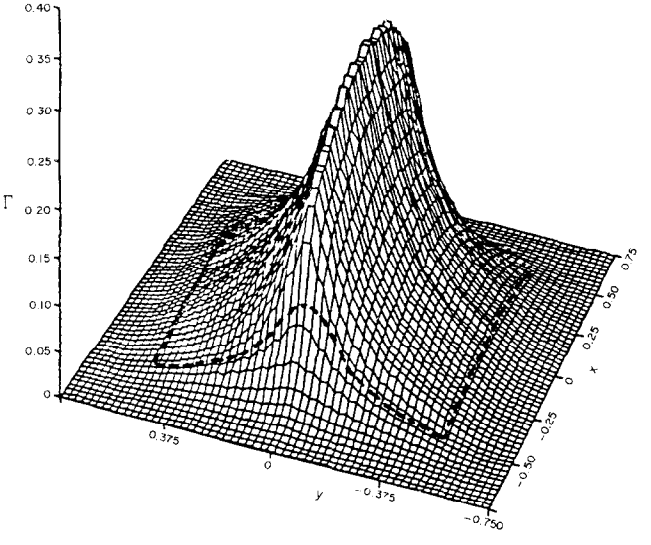

FIG. 6. Numerically reconstructed dimensionless temperature (Γ) distribution in a horizontal plane containing the centerline of the cylinder. $Ra_H = 3.98 \times 10^4$, $Pr = 261$, $A_r = 1.0$.

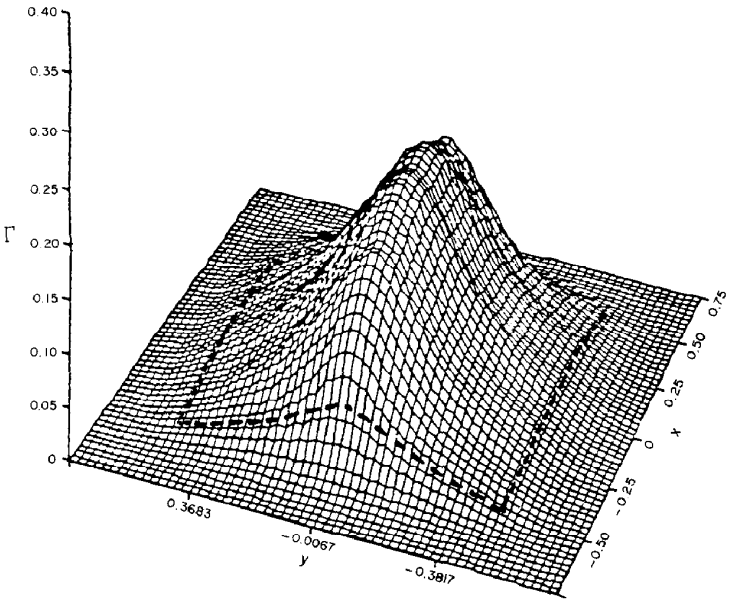

FIG. 7. Numerically reconstructed dimensionless temperature distribution in a horizontal plane 0.1 cylinder diameters below the centerline of the cylinder.

mation, the largest reconstruction grid which gave meaningful results and yet had sufficient data redundancy was a 9×9 grid centered around the cylinder and having a grid spacing of 0.25 cylinder diameters. Figure 8 shows the temperature field together with a dotted line that indicates the solid–liquid interface. Similar to the numerical reconstruction shown in Fig. 7, it may be observed that the temperature in Fig. 8 is highest along the cylinder centerline where the heat source is located. In spite of the jagged nature of the experimental result, the qualitative agreement between the experimentally reconstructed temperature field and the numerical solution may be seen to be good and must be viewed in light of the fact that there were several sources of experimental errors which will be outlined later.

Figure 9 shows the isotherms in the fluid in the horizontal plane 0.595 diameters above the centerline

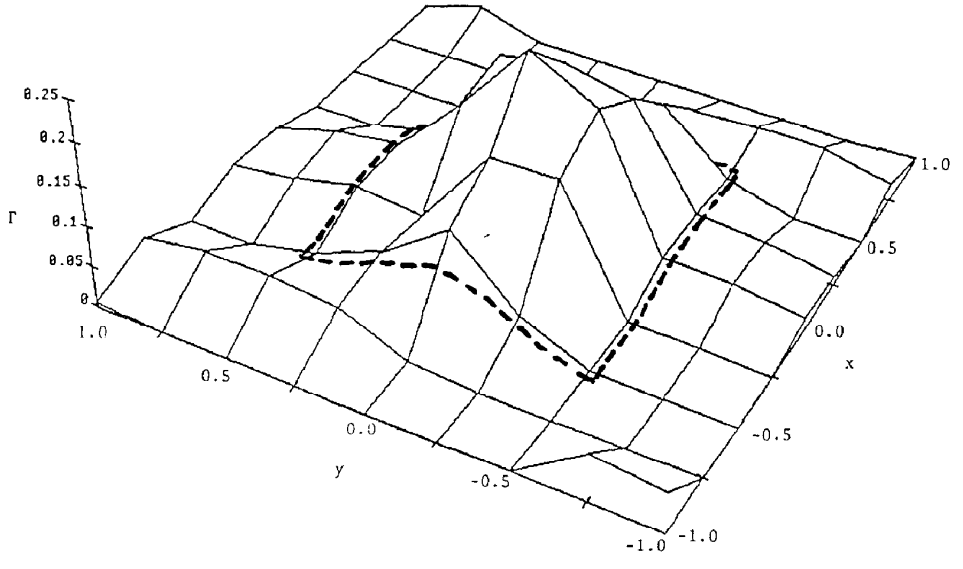

FIG. 8. Experimentally reconstructed dimensionless temperature distribution in a horizontal plane 0.1 cylinder diameters below the centerline of the cylinder.

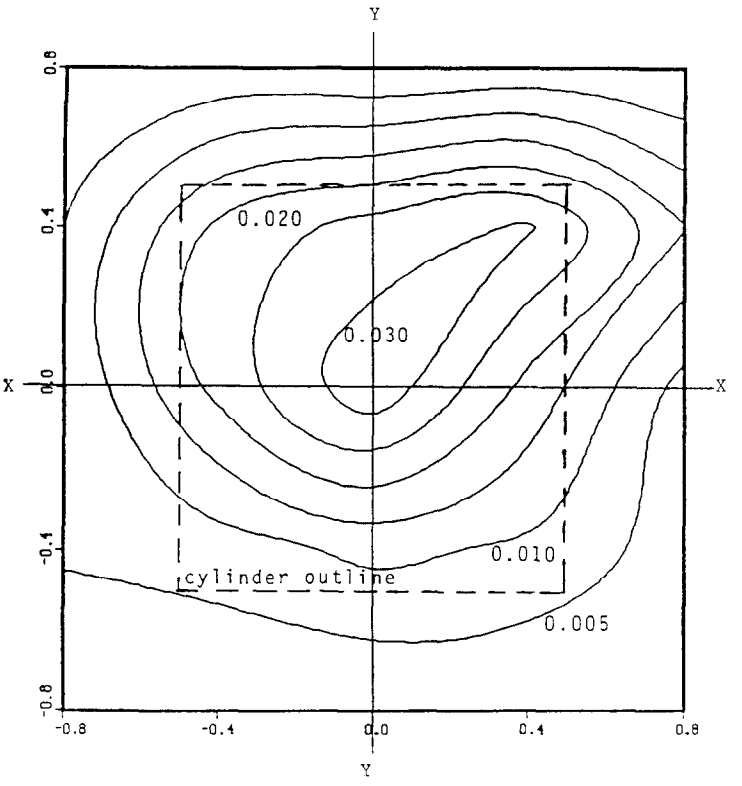

FIG. 9. Experimentally measured isotherms (non-dimensional temperature Γ) in the fluid in a horizontal plane 0.595 cylinder diameters above the centerline of the cylinder, $Ra_q = 3.98 \times 10^4$, $Pr = 261$, $A_r = 1.0$.

of the cylinder. Pathlength data were used along five angles of view—20, 30, 50, 60 and 70 deg with respect to the axis of the cylinder. There were, on the average, 20 points per view. The outline of the cylinder as viewed from this plane is shown in Fig. 9 as well. An interesting observation is that the temperature field is skewed to one side. The highest temperature in the cross-section is not directly above the center of the cylinder, but is shifted towards the upper right-hand corner. From the fringe patterns, it was observed that the plume is not symmetric about either the XX or the YY axis of the cylinder. A portion of the heater wire (placed along the centerline of the cylinder XX) extended further out on one end of the cylinder than the other. This caused asymmetric heating of the solid with the plume having a preferred direction towards the side of the cylinder with higher heating.

The experimentally reconstructed and the numerically calculated temperature distributions were compared along a line in the fluid above the cylinder. Figure 10 shows the temperature variation along a line in the x-direction in the plane $z = 0.6$ at the location $y = 0.120$. The numerical solution is symmetric about the midplane whereas the skewed experimental temperature distribution is evident. In spite of this, the agreement between the two is quite good.

An error analysis of the data was made in an effort to determine the uncertainty in the experimentally determined temperature. The inability to identically replicate the bulk fluid conditions before and after heating the cylinder caused a shift in the infinite field fringes and represented the largest source of uncertainty. The uncertainty in locating the center of the cylinder in the digitized fringe pattern also contributed to the uncertainty. Errors associated with the inversion algorithm were detailed in an earlier section. Another component of the uncertainty is the refraction error caused by bending the light beam near the cylinder where the refractive index gradient is the largest. A combination of all these sources of error gave an overall uncertainty in the temperature measurement of approximately 16% of the maximum non-dimensional cylinder temperature (Γ). Considering this, the agreement between the numerical solutions and experimental data is indeed quite good.

SUMMARY

An optical technique has been devised for the measurement of a 3-D temperature field in a region containing both a solid and a fluid using an interferometric method. The geometry chosen for testing the technique was a horizontal cylinder (aspect ratio of unity) with a line heat source along its centerline placed in a fluid of matched index of refraction to which heat is transferred by laminar natural convec-

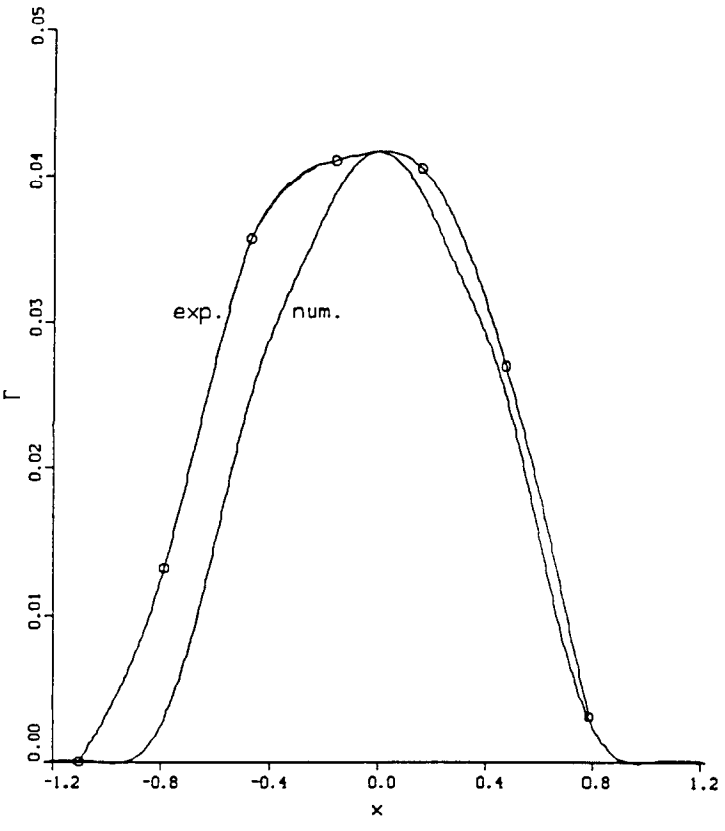

FIG. 10. Comparison between the experimentally and numerically obtained non-dimensional temperature distribution in the plume in the x-direction at $y = 0.120$ and $z = 0.60$.

tion. This selection was made because of ease of fabrication and it also served the purpose of providing a 3-D temperature distribution with thick boundary layers. Before taking experimental data, several mathematical reconstruction algorithms were evaluated to determine their applicability. Selection criteria were mainly simplicity, versatility and ease of implementation. Using the general code developed in ref. [16], a numerical solution was obtained for this problem. The temperature field in horizontal planes containing the solid was integrated to generate simulated pathlength data and used for testing the inversion algorithm. The error in the reconstructed temperature field was obtained directly. The Grid method which had an average reconstruction error of 3% was chosen as the best reconstruction method for use here.

Experiments were performed with a Plexiglas cylinder placed in a fluid (dibutylphthalate) having a matched index of refraction. Interferograms of the temperature field were recorded at ten different angular orientations of the cylinder. The temperature field was reconstructed in horizontal planes above and also through the cylinder. The uncertainty in the temperature determination was estimated to be nearly 16% of the difference between the highest temperature above the cylinder and the bulk fluid. The temperature fields in the fluid and the solid obtained from the experiments were compared with corresponding numerical results. They were found to be in excellent agreement and well within the limits of uncertainty in the experiments.

Some of the difficulties faced with the present interferometer in obtaining the temperature field within the solid could have been eliminated if a holographic system was employed. A double exposure technique can be used in which the hologram is exposed initially before the temperature field is established, and then it is exposed again in the presence of the temperature field. This would optically subtract the noise, particularly in the solid region. Also, if suitably arranged, data along various angles of view can be recorded simultaneously for the study of transient flows.

Acknowledgements—This research was supported by the National Science Foundation through grant (BT-8313629. A grant for computer time on the Cray-2 from the Supercomputer Institute of the University of Minnesota is also gratefully acknowledged.

REFERENCES

1. E. R. G. Eckert and E. Soehngen, Manufacture of a Zehnder–Mach interferometer, U.S. Airforce Tech. Report 5721, Wright Patterson AFB, Dayton (1947).
2. E. R. G. Eckert and E. Soehngen, Studies on heat transfer in laminar free convection with the Zehnder–Mach

interferometer, U.S. Airforce Tech. Report 5747, Dayton (1948).
3. W. Hauf and U. Grigull, Optical methods in heat transfer. In *Advances in Heat Transfer*, Vol. 6, pp. 133–366, Academic Press, New York (1970).
4. R. N. Bracewell and A. C. Riddle, Inversion of fan-beam scans in radio astronomy, *Astrophys. J.* **150**, 427–434 (1967).
5. R. Gordon, R. Bender and G. T. Herman, Algebraic reconstruction techniques (ART) for three-dimensional electron microscopy and X-ray photography, *J. Theor. Biol.* **29**, 471–481 (1970).
6. P. D. Rowley, Quantitative interpretation of three-dimensional weakly refractive phase objects using holographic interferometry, *J. Opt. Soc. Am.* **59**, 1496–1498 (1969).
7. D. W. Sweeney and C. M. Vest, Reconstruction of three-dimensional refractive index fields from multidirectional interferometric data, *Appl. Optics* **12**, 2649–2664 (1973).
8. C. M. Vest, Tomography for properties of materials that bend rays: a tutorial, *Appl. Optics* **24**, 4089–4094 (1985).
9. R. D. Matulka and D. J. Collins, Determination of three-dimensional density fields from holographic interferograms, *J. Appl. Phys.* **42**, 1109–1119 (1971).
10. H. H. Chau and O. S. F. Zucker, Holographic thin beam reconstruction technique for the study of a 3-D refractive index field, *Opt. Commun.* **8**, 336–339 (1973).
11. C. M. Vest and P. T. Radulovic, Measurement of three-dimensional temperature fields by holographic interferometry. In *Application of Holography and Optical Data Processing*, pp. 241–249, Pergamon Press, London (1977).
12. D. W. Sweeney and C. M. Vest, Measurement of three-dimensional temperature fields above heated surfaces by holographic interferometry, *Int. J. Heat Mass Transfer* **17**, 1443–1454 (1974).
13. H. Oertel, Three-dimensional convection within rectangular boxes. In *Natural Convection in Enclosures, Proc. 19th Natn. Heat Transfer Conf.* (July 1980).
14. F. Mayinger and D. Lubbe, Ein Tomographisches Meßverfahren und Seine Anwendung auf Mischvorgange und Stoffaustausch, *Wärme- und Stöffubertr.* **18**, 49–59 (1984).
15. D. Mewes and W. Ostendorf, Application of tomographic measurement techniques for process engineering studies, *Int. Chem. Engng* **26**, 11–21 (1986).
16. A. K. Tolpadi and T. H. Kuehn, Computation of three-dimensional natural convection heat transfer from a transversely finned horizontal cylinder, *Numer. Heat Transfer* **16A**, 1–13 (1989).
17. A. K. Tolpadi, Coupled three-dimensional conduction and natural convection heat transfer, Ph.D. Thesis, University of Minnesota (1987).

MESURE PAR INTERFEROMETRIE MULTIDIRECTIONNELLE DES CHAMPS TRIDIMENSIONNELS DE TEMPERATURE DANS DES PROBLEMES CONJUGUES DE CONDUCTION–CONVECTION

Résumé—Une étude numérique et expérimentale est conduite pour observer optiquement et reconstruire un champ tridimensionnel (3D) de température dans des problèmes de transfert thermique couplé de conduction–convection. La distribution de température peut être obtenue dans le solide conducteur et le fluide adjacent qui convecte. Un algorithme de reconstruction donne le champ de température 3D dans une region occupée par des milieux multiples (solides et/ou fluides). La distribution 3D de température est reconstruite dans et autour d'un cylindre court et chaud placé dans un fluide auquel la chaleur est transférée par convection naturelle. La mesure expérimentale du champ est faite par enregistrement et réduction des données à partir d'interférogrammes pris selon différents angles de l'écoulement. Des solutions numériques pour cette géométrie sont obtenues qui donnent les champs de température lesquels se comparent favorablement aux valeurs obtenues expérimentalement.

MESSUNG DREIDIMENSIONALER TEMPERATURFELDER MIT HILFE DER MULTIDIMENSIONALEN INTERFEROMETRIE BEI KONJUGIERTEN LEITUNGS/KONVEKTIONSPROBLEMEN

Zusammenfassung—In der vorliegenden numerischen und experimentellen Untersuchung wird das asymmetrische dreidimensionale Temperaturfeld bei konjugierten Wärmeleitungs/Konvektions-Problemen optisch aufgezeichnet und rekonstruiert. Bei einer thermisch gekoppelten Anwendung muß die Temperaturverteilung innerhalb des wärmeleitenden Festkörpers und im umgebenden bewegten Fluid ermittelt werden. Hierzu wird ein Rekonstruktionsalgorithmus entwickelt, der das dreidimensionale Temperaturfeld in einem Gebiet berechnet, das durch mehrere Medien (Festkörper und/oder Fluide) besetzt ist. Die dreidimensionale Temperaturverteilung wird in und um einen kurzen beheizten Zylinder in einem Fluid bestimmt, dem Wärme durch natürliche Konvektion zugeführt wird. Eine Reihe von Interferogrammen werden unter verschiedenen Winkeln zur Strömung aufgenommen. Um Interferenzwerte für die Kombination aus Festkörper und Fluid zu erhalten, wird die Brechzahl des Zylinders derjenigen des Fluides angepaßt. Die für diese geometrische Anordnung numerisch ermittelten Temperaturfelder stimmen gut mit den experimentellen Werten überein.

ИЗМЕРЕНИЕ ТРЕХМЕРНЫХ ТЕМПЕРАТУРНЫХ ПОЛЕЙ В СВЯЗАННЫХ ЗАДАЧАХ ТЕПЛОПРОВОДНОСТИ-КОНВЕКЦИИ С ИСПОЛЬЗОВАНИЕМ МНОГОНАПРАВЛЕННОЙ ИНТЕРФЕРОМЕТРИИ

Аннотация—Проводятся численные и экспериментальные исследования с целью оптической регистрации и восстановления асимметричного трехмерного температурного поля в связанных задачах кондуктивно–конвективного теплообмена. Для решения тепловой задачи температурное распределение должно определяться в твердом теле и в прилегающей жидкости, в которой происходит конвекция. Разработан алгоритм восстановления, позволяющий определить трехмерное температурное поле в области, занимаемой различными средами (твердые тела и/или жидкости). Трехмерное распределение температур восстанавливается внутри и вокруг короткого нагретого цилиндра, помещенного в жидкость, в которую тепло переносится естественной конвекцией. Экспериментальное измерение поля проводится посредством регистрации и преобразования данных из ряда интерферограмм, снимаемых под разными углами к потоку. Получены численные решения для рассматриваемой геометрии, на основе которых определены температурные поля, удовлетворительно согласующиеся с экспериментальными данными.